Transaction A: Civil Engineering
Vol. 16, No. 3, pp. 256–263

SCIENTIA IRANICA

Semi-Active Control of Structures Using a Neuro-Inverse Model of MR Dampers

A. Khaje-Karamodin[1], H. Haji-Kazemi[1,*], A.R. Rowhanimanesh[2] and M.R. Akbarzadeh-Tootoonchi[2]

Abstract. *A semi-active controller-based neural network for a 3 story nonlinear benchmark structure equipped with a Magneto Rheological (MR) damper is presented and evaluated. An inverse neural network model (NIMR) is constructed to replicate the inverse dynamics of the MR damper. A Linear Quadratic Gaussian (LQG) controller is also designed to produce the optimal control force. The LQG controller and the NIMR models are linked to control the structure. The effectiveness of the NIMR is illustrated and verified using the simulated response of a full-scale, nonlinear, seismically excited, 3-story benchmark building excited by several historical earthquake records. The semi-active system using the NIMR model is compared to the performance of an active LQG and a Clipped Optimal Control (COC) system, which is based on the same nominal controller as used in the NIMR damper control algorithm. Two passive control systems are also considered and compared. The results demonstrate that by using the NIMR model, the MR damper force can be commanded to follow closely the desirable optimal control force. The results also show that the control system is effective, and achieves better performance than active LQG and COC system. The optimal passive controller performs better than the NIMR. However, the performance of NIMR will be improved if a more effective active controller is replaced by a LQG controller.*

Keywords: *Structural control; Semi-active; Neural network; Nonlinear; MR damper.*

INTRODUCTION

The Magneto Rheological (MR) damper is generating a great interest among researchers in the semi-active control of civil structures [1-4]. The MR damper is a smart semi-active control device that generates force to a given velocity and applied voltage. The MR damper is filled with a special fluid that includes very small polarizable particles, which can change its viscosity rapidly from liquid to semi-solid and vice versa by adjusting the magnitude of the magnetic field produced by a coil wrapped around the piston head of the damper. The magnetic field can be tuned by varying the electrical current sent into the coil. When no current is supplied, the MR damper behaves similar to an ordinary viscous damper, whereas its fluid starts to change to semi-solid as the current is gradually sent through the coil. Consequently, semi-active controllers using MR dampers are powerful devices that enjoy the advantages of passive devices with the benefits of active control. Additionally, they are inherently stable, reliable and relatively cost-effective and require small activation power.

One challenge in the use of semi-active technology is in developing nonlinear control algorithms that are appropriate for implementation in full-scale structures. Numerous control algorithms have been adopted for semi-active systems. These algorithms are either conventional methods based on mathematical formulation [1-4] or intelligent methods based on neural networks or fuzzy logic [5-7].

Interest in a new class of computational intelligence systems known as Artificial Neural Networks (ANNs) has grown in the last few years. This type of network has been found to be a powerful computational tool for organizing and correlating information in ways that have been proven to be useful for

1. *Department of Civil Engineering, Ferdowsi University of Mashhad, Mashhad, P.O. Box 9177948944-1111, Iran.*
2. *Department of Electrical Engineering, Ferdowsi University of Mashhad, Mashhad, P.O. Box 9177948944-1111, Iran.*
*. *Corresponding author. E-mail: hkazemi@ferdowsi.um.ac.ir*

Received 20 November 2007; received in revised form 9 August 2008; accepted 1 November 2008

solving certain types of problem that are complex and poorly understood. The applications of ANNs to the area of structural control have grown rapidly through system identification, system inverse identification or controller replication [5-6].

In addition to using the Linear Quadratic Regulator (LQR) method, Chang and Zhou [8] manipulated recurrent neural networks to emulate the inverse dynamics of the MR damper to predict the required voltage for a full-state feedback closed-loop system. This model was used to control a three-storey building subjected to the El Centro earthquake record. Similarly, Bani-Hani et al. [5] proposed neural network to simulate the inverse model of an MR damper in a 6-story base-isolated building subjected to earthquake forces.

In this paper, a NN model is used to emulate the inverse dynamics of the MR damper. This NN model (NIMR) is trained based on the input-output data generated using the phenomenological model proposed by Dyke et al. [9]. The model calculates a voltage signal based on a few previous time steps of velocity, damper force and desirable control force. This NN model is used to calculate voltage signals to be input to the MR damper so that it can produce desirable optimal control forces that are estimated by the LQG control algorithm. In principle, these control forces can come from any control algorithm that requires an explicit use of control forces to mitigate response. The effectiveness of the NIMR is illustrated and verified using the simulated response of a full-scale, nonlinear, seismically excited, 3-story benchmark building excited by several historical earthquake records. The semi-active system using the NIMR model is compared to the performance of an active LQG and a Clipped Optimal Control (COC) system, which are based on the same nominal controller used in the NIMR control algorithm. Additionally, two passive control systems are also considered and compared.

THREE-STORY BENCHMARK BUILDING

The benchmark 3-story building used for this study was designed for the Los Angeles region, as defined by Ohtori et al. [10] in the problem definition paper. The building is 36.58 m by 54.87 m in plan and 11.89 m in height. Two far-field and two near-field historical ground motion earthquake records are selected for study: El Centro (1940), Hachinohe (1968), Northridge (1994) and Kobe (1995). Control actuators are located on each floor of the structure to provide forces to adjacent floors. Because the actuator capacity is limited to a maximum force of 1,000 kN, three actuators are employed at the first floor and two actuators at both the second and the third floors to provide the required larger forces. Three sensors for acceleration measurements are used for feedback in the control system on the first, second and third floors.

CONTROL STRATEGY

Figure 1 illustrates the proposed control strategy. There is basically no restriction on the type of control algorithm that should be used, as long as it calculates a desirable control force, f_d, based on response and/or excitation. The desirable control force and the response of the building are passed into the inverse NN model. This NN model emulates the inverse dynamics of the MR damper. The output of this inverse NN model is the voltage required to produce the desirable control force under the current response condition. This voltage is input to the MR damper, which then produces force facting on the building.

MR Model

Adequate modeling of the control devices is essential for accurate prediction of the behavior of the controlled system. The simple mechanical model shown

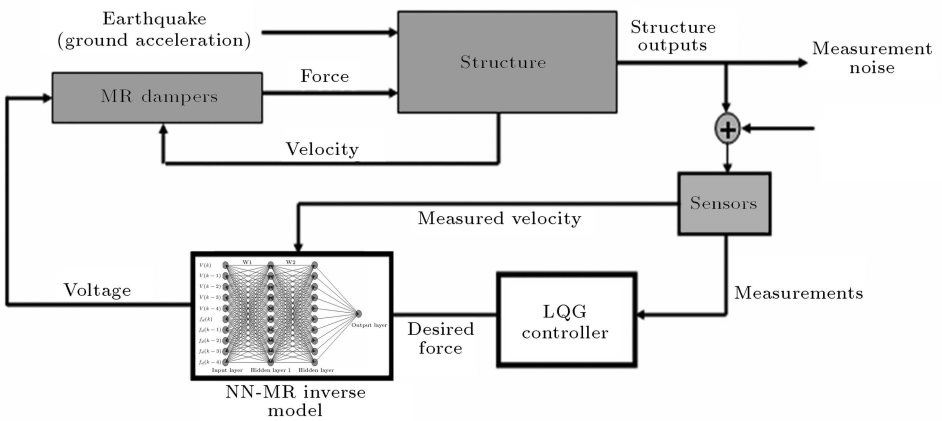

Figure 1. Control strategy.

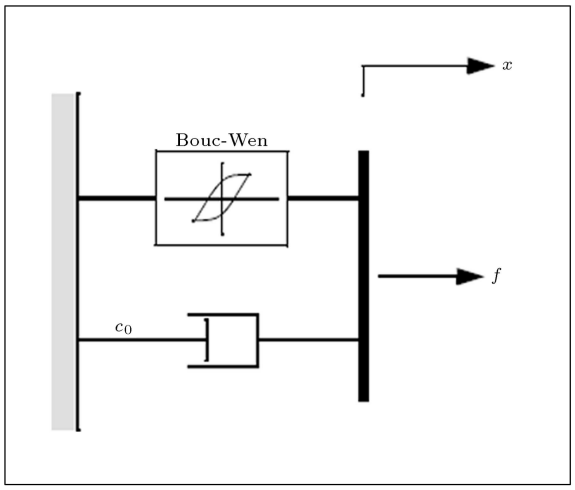

Figure 2. Mechanical model of MR damper.

in Figure 2 was developed and shown to accurately predict the behavior of the MR damper over a wide range of inputs [9]. This phenomenological model was developed based on a previous model used for a MR damper [11]. The equations governing the force, f, predicted by this model are as follows:

$$f = c_0\dot{x} + \alpha z, \tag{1}$$

$$\dot{z} = -\gamma|\dot{x}|z|z|^{n-1} - \beta\dot{x}|z|^n + A\dot{x}, \tag{2}$$

where z is the evolutionary variable that accounts for the history dependence of the response. The model parameters depend on the voltage, v, to the current driver as follows:

$$\alpha = \alpha_a + \alpha_b u, \tag{3a}$$

$$c_0 = c_{0a} + c_{0b} u, \tag{3b}$$

where u is given as the output of the first-order filter:

$$\dot{u} = -\eta(u - v). \tag{4}$$

Equation 4 is used to model the dynamics involved in reaching rheological equilibrium and in driving the electromagnet in the MR damper [9]. This MR damper model is used herein to model the behavior of the MR damper. The parameters of the MR damper were selected so that the device has a capacity of 1,000 kN, as follows:

$\alpha_a = 1.0872e5$ N/cm,

$\alpha_b = 4.9616e5$ N/(cm V),

$c_{0a} = 4.40$ N s/cm,

$c_{0b} = 44.0.$ N s/(cm V),

$n = 1, \qquad A = 1.2, \qquad \gamma = 3\ \text{cm}^{-1},$

$\beta = 3\ \text{cm}^{-1}, \qquad \gamma = 50\ \text{s}^{-1}.$

Neural Network Inverse Dynamics of MR Damper (NIMR)

The MR damper model discussed earlier in this paper estimates damper forces based on the inputs of the reactive velocity and the issued voltage as described by Equations 1 to 4. The damper velocity is the same as the velocity of the floor to which the damper is connected. Thus, the voltage signal is the only parameter that can be modified to control the damper force to produce the required control force. The control algorithm, LQG, estimates the required optimal control force but the MR damper force is controlled by voltage. In such a case, it is essential to develop an inverse dynamic model that predicts the corresponding control voltage to be sent to the damper, so that an appropriate damper force can be generated. Unfortunately, due to the inherent nonlinear nature of the MR damper, a mathematical model for its inverse dynamics is difficult to obtain. Because of this reason, a feed-forward back-propagation neural network is constructed to copy the inverse dynamics of the MR damper (Figure 3). This model is denoted as NIMR. This neural network model is trained using input-output data generated analytically using the simulated MR model based on Equations 1 to 4. This NIMR calculates the voltage signal based on the current and few previous histories of measured velocity and desirable control force. Then, the voltage signals are sent to the MR damper so that it can generate the desirable optimal control forces.

Training the NIMR requires the compilation of input-output data. To completely identify the underlying MR system model, the data must contain information about the entire operating range of the system. Here, in this study, the velocity and voltage are generated randomly using band limited white Gaussian noise. The generated forces are results of the MR model described in Equations 1 to 4. The sampling rate of the training data was 200 Hz for 30 s periods,

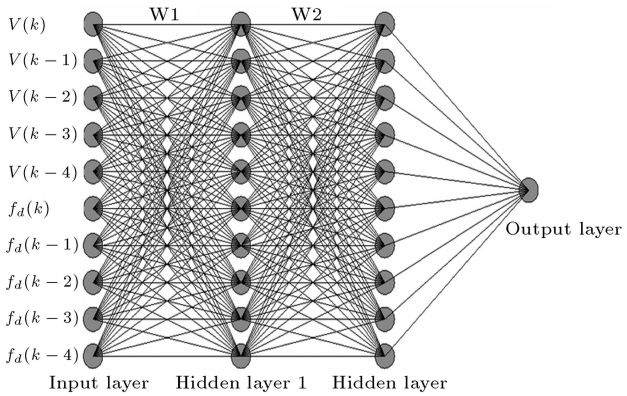

Figure 3. NN of inverse dynamics of MR damper (NIMR).

which resulted in 6000 patterns for training, testing and validation (Figure 4). The next step is to select the network architecture. To do so, it is required to determine the numbers of inputs, outputs, hidden layers and nodes in the hidden layers, which is usually done by trial and error. The most suitable input data for our case was found to be the current and four previous histories for the velocity and the force. Also, two hidden layers, each layer with ten nodes, were adopted as one of the best suitable topologies for the NIMR, as can be seen in Figure 3. The log-sigmoid (ranging from 0 to 1) activation function is used for the hidden layers and the linear function for the output layer, which represents the voltage. 3000 patterns of the provided data were chosen for training which required 1000 training epochs to achieve a Mean-Square-Error (MSE) of 1e-03.

The training is carried out upon the generated data using the Levenberg-Marquardt algorithm [12], which is encoded in Neural Networks Toolbox in MATLAB [13] under the 'trainlm' routine. Finally, testing and validation of the trained network is investigated using a few sets of new data for a 30 s period. Figure 5 shows the training testing and validation velocity, forces and voltage records used in constructing the NIMR model. Additionally, Figure 5 compares the forces computed by the MR damper model based on the generated random voltage to the forces computed by the MR damper model based on the predicted voltages by NIMR. Moreover, the predicted voltage record from the NIMR is compared to the randomly generated targets and presented in Figure 5. It is clear that, in general, the predicted voltages are reasonably close to the target voltages. The near perfect match in the training region indicates that the NIMR model is well trained. Henceforth, the NIMR model will be used to compute the required voltage for a specific force and velocity. This will alleviate problems resulting when using a control algorithm that computes only the optimal control forces.

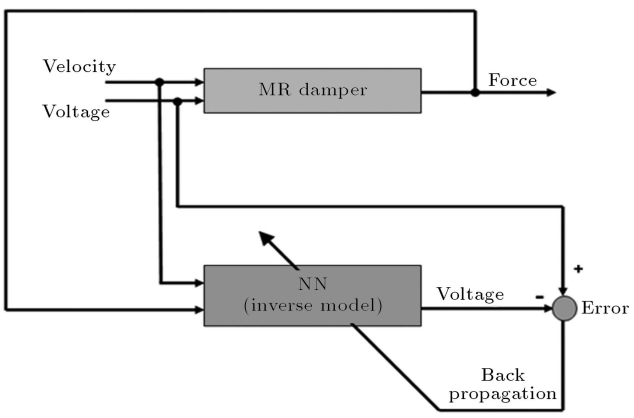

Figure 4. Training of NIMR.

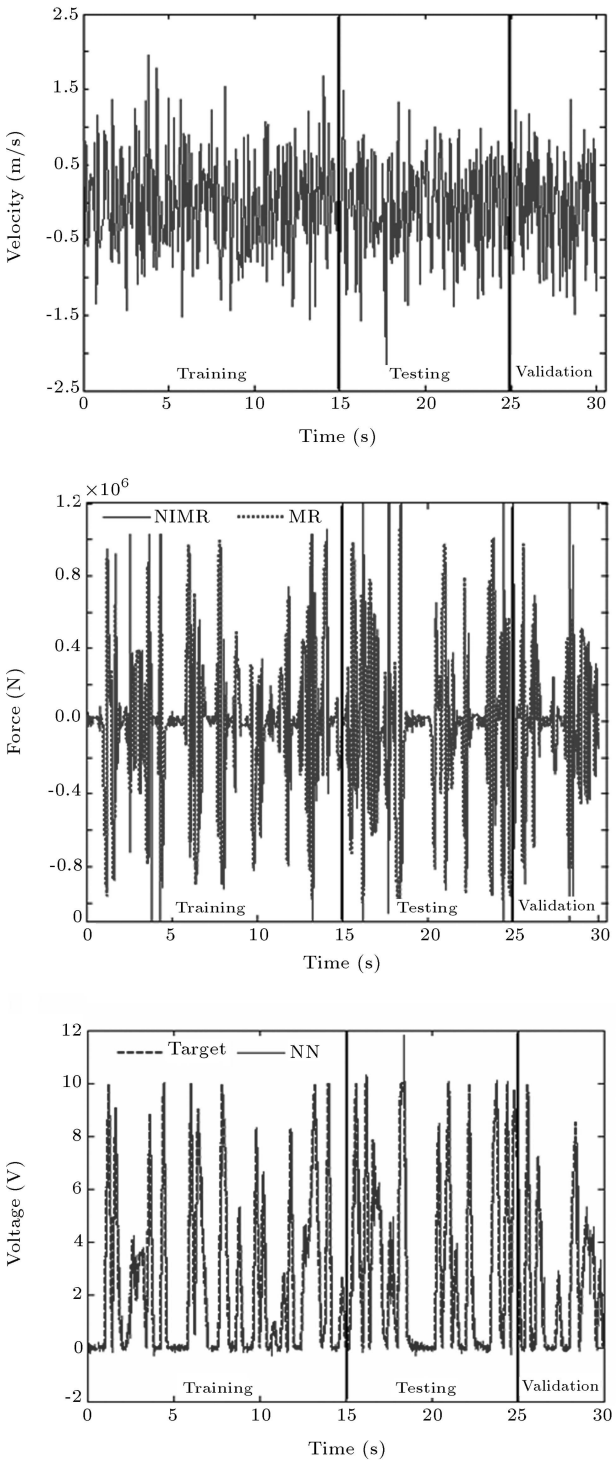

Figure 5. Training, testing and validation data.

Control Performance

The performance of the NIMR neural network is checked according to comparison of the force generated by the MR damper to the ideal force estimated by the LQG controller. Figure 6 shows the force generated by the MR damper at the first floor of the building for the El Centro earthquake, commanded by

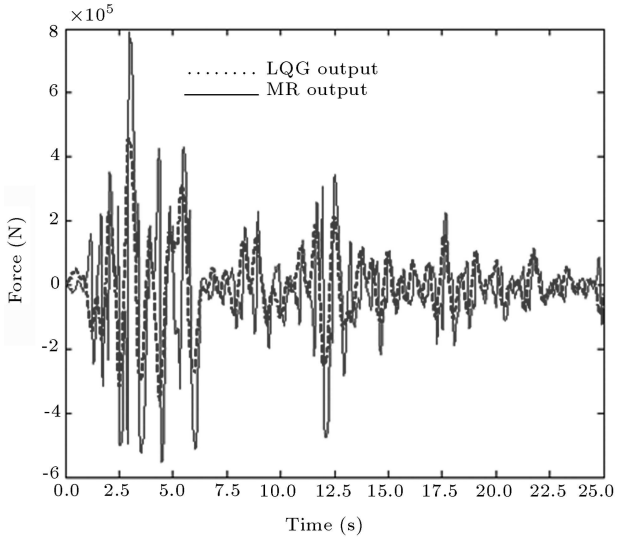

Figure 6. Comparison of the force generated by MR damper to the ideal force (LQG).

NIMR, as compared to the ideal force estimated by the LQG controller. It can be seen that the damper forces follow the target optimal control force quite closely.

The performance of the controller is also investigated based on the evaluation criteria specified (J1-J6) for the 3-story nonlinear benchmark building [10]. These criteria, which are briefly presented in Table 1, are calculated as a ratio of the controlled and the uncontrolled responses, in most cases. Ten earthquake records are used in the simulation, using the original four earthquake records with different intensities. These records are the El Centro and Hachniohe earthquake records with 0.5, 1.0, and 1.5 intensity and Northridge and Kobe earthquake records with 0.5 and 1.0 intensity. To make a comparison, an active control system and semi-active Clipped-Optimal Control (COC) system [4] are also designed. Moreover, to compare the performance of the proposed method, two passive control systems have been considered. Both passive control systems use the MR damper in passive mode (constant voltage). The first passive system designated as Passive On (PON) uses the MR damper with maximum voltage (10 Volts). In the second passive system, named Optimal Passive Control (OPC), the voltage of the MR damper in each story is defined as an optimization problem. The objective of the optimization is to minimize the average of the performance indices, J1-J6, under the El Centro earthquake. Table 2 presents the evaluation criteria as the ratio of the controlled response to the uncontrolled response for each earthquake record, individually, for active LQG, COC, PON, OPC and the proposed control algorithms. Figure 7 also shows the relative performance of these algorithms for criteria J1, J2, J3, J4, J5 and J6. The results show that the NIMR controller performs better than COC and active control in reducing the peak drift ratio (J1). For the peak level acceleration (J2), the NIMR controller has been able to perform better than COC, but the LQG controller is more effective. The peak base shear force criterion (J3) for NIMR is smaller than COC but greater than active LQG. In terms of norm drift ratio (J4), the performance of NIMR is better than COC and LQG. The NIMR is more effective than COC and LQG in the reduction of norm level acceleration (J5) and the norm base shear force (J6). The results also show that PON performs better to reduce the drift, but increases the acceleration of the building. It is also seen that OPC performs better than other controllers to reduce the drift and acceleration of the building. However, it should be noted that the primary controller used in the proposed semi-active control method (LQG) is the optimal controller for linear systems. The 3 story building in this paper is a nonlinear system and the LQG controller is not an optimal controller for this building. So, if a more effective active controller is used as a primary controller, the semi-active controller will be more effective.

CONCLUSION

In this study, neural networks are used to model the inverse dynamics of MR damper. The inputs to the NN models are a few time steps of structural velocities and damper forces. The output is the command voltage

Table 1. Performance criteria for seismically excited nonlinear building.

Interstory Drift Ratio	**Level Acceleration**	**Base Shear**
$J_1 = \max_{\substack{\text{El centro}\\ \text{Hachino}\\ \text{Northridge}\\ \text{Kobe}}} \left\{ \frac{\max_{t,i} \frac{\lvert d_i(t)\rvert}{h_i}}{\delta^{\max}} \right\}$	$J_2 = \max_{\substack{\text{El centro}\\ \text{Hachino}\\ \text{Northridge}\\ \text{Kobe}}} \left\{ \frac{\max_{t,i} \lvert \ddot{x}_{ai}(t)\rvert}{\ddot{x}_{ai}^{\max}} \right\}$	$J_3 = \max_{\substack{\text{El centro}\\ \text{Hachino}\\ \text{Northridge}\\ \text{Kobe}}} \left\{ \frac{\max_t \left\lvert \sum_i m_i \ddot{x}_{ai}(t) \right\rvert}{F_b^{\max}} \right\}$
Normed Interstory Drift Ratio	**Normed Level Acceleration**	**Normed Base Shear**
$J_4 = \max_{\substack{\text{El centro}\\ \text{Hachino}\\ \text{Northridge}\\ \text{Kobe}}} \left\{ \frac{\max_{t,i} \frac{\lVert d_i(t)\rVert}{h_i}}{\lVert \delta^{\max} \rVert} \right\}$	$J_5 = \max_{\substack{\text{El centro}\\ \text{Hachino}\\ \text{Northridge}\\ \text{Kobe}}} \left\{ \frac{\max_{t,i} \lVert \ddot{x}_{ai}(t)\rVert}{\lVert \ddot{x}_a^{\max} \rVert} \right\}$	$J_6 = \max_{\substack{\text{El centro}\\ \text{Hachino}\\ \text{Northridge}\\ \text{Kobe}}} \left\{ \frac{\max_i \left\lVert \sum_i m_i \ddot{x}_{ai}(t) \right\rVert}{\lVert F_b^{\max} \rVert} \right\}$

Table 2. Performance criteria for active, Clipped Optimal Control (COC), NIMR, PON and OPC algorithms.

	Controller	El-Centro 0.5	El-Centro 1	El-Centro 1.5	Hachino 0.5	Hachino 1	Hachino 1.5	North-ridge 0.5	North-ridge 1	Kobe 0.5	Kobe 1	Average
	NIMR	0.406	0.575	0.807	0.592	0.689	0.736	0.583	0.874	0.876	0.603	0.674
	COC	0.457	0.704	0.883	0.541	0.697	0.706	0.714	0.950	0.881	0.752	0.728
J1	Active	0.544	0.753	0.873	0.637	0.768	0.794	0.826	1.035	0.819	0.854	0.790
	PON	0.271	0.476	0.717	0.155	0.212	0.358	0.392	0.761	0.724	0.715	0.478
	OPC	0.376	0.565	0.875	0.187	0.420	0.590	0.554	0.845	1.013	0.692	0.612
	NIMR	0.548	0.712	0.943	0.777	0.903	1.108	0.875	1.060	0.933	0.791	0.865
	COC	0.820	0.829	0.938	0.812	0.909	0.957	0.862	0.890	0.871	1.002	0.889
J2	Active	0.598	0.781	0.939	0.658	0.798	0.844	0.851	0.869	0.829	0.833	0.800
	PON	0.649	0.881	1.142	0.721	0.439	0.738	0.795	1.019	1.102	0.800	0.829
	OPC	0.712	0.829	1.041	0.376	0.628	1.029	0.883	0.974	0.931	0.752	0.816
	NJMR	0.452	0.817	1.037	0.518	0.733	0.954	0.978	1.057	0.958	0.945	0.845
	COC	0.583	1.043	1.062	0.574	0.797	0.923	0.910	0.943	0.994	1.006	0.883
J3	Active	0.507	0.881	0.914	0.553	0.779	0.925	0.831	0.819	0.851	0.966	0.803
	PON	0.614	0.868	1.083	0.522	0.609	0.834	0.716	1.014	1.098	1.091	0.845
	OPC	0.501	0.856	1.124	0.453	0.701	0.979	0.851	1.028	1.045	1.017	0.856
	NIMR	0.652	0.655	0.654	0.460	0.442	0.736	0.173	0.662	1.525	1.050	0.701
	COC	0.656	0.776	0.693	0.352	0.471	0.956	0.710	1.199	1.149	1.576	0.854
J4	Active	0.799	0.851	0.708	0.590	0.655	1.199	1.088	1.237	0.829	1.202	0.916
	PON	0.258	0.346	0.378	0.166	0.151	0.189	0.108	1.120	0.617	0.274	0.361
	OPC	0.292	0.411	0.483	0.135	0.170	0.220	0.102	1.133	1.374	0.930	0.525
	NIMR	0.754	0.838	0.881	0.523	0.543	0.626	0.828	0.906	0.743	0.878	0.752
	COC	0.781	0.945	0.932	0.570	0.565	0.704	0.861	0.887	0.794	0.915	0.795
J5	Active	0.764	0.931	0.925	0.561	0.685	0.814	0.878	0.914	0.821	0.926	0.822
	PON	4.066	2.385	1.744	3.125	1.775	1.445	3.333	2.295	2.703	2.147	2.502
	OPC	0.983	0.682	0.704	0.749	0.512	0.468	0.919	0.770	0.762	0.722	0.727
	NIMR	0.367	0.413	0.435	0.267	0.278	0.323	0.469	0.482	0.368	0.459	0.386
	COC	0.377	0.466	0.456	0.230	0.289	0.361	0.481	0.474	0.396	0.468	0.400
J6	Active	0.370	0.455	0.446	0.279	0.341	0.407	0.476	0.468	0.390	0.455	0.409
	PON	1.292	1.117	1.058	0.906	0.729	0.720	1.268	1.130	1.062	1.198	1.048
	OPC	0.691	0.707	0.716	0.433	0.391	0.434	0.687	0.721	0.619	0.729	0.613

to the MR damper. These NN models estimate the voltage that is required to produce a target control force calculated from some optimal control algorithms. The main objective of this development is to explore whether the semi-active MR damper can be used to produce optimal control forces.

A 3-story nonlinear benchmark building has been used for study. The results illustrate that it is possible to incorporate the NN models into the control strategy and, hence, operate the damper in an active mode. In general, the forces generated by the MR damper can follow those caculated from the optimal control algorithms. The performance of the controller has been checked, based on the evaluation criteria specified (J1-J6) for the benchmark building. The results show that the mean of the average indices, J1 to J6, for different earthquake records are 0.768, 0.825, 0.825, 1.010 and 0.691, respectively, for NIMR, COC, LQG, PON and OPC methods. It can be concluded that the NIMR controller performs better than the COC, LQG

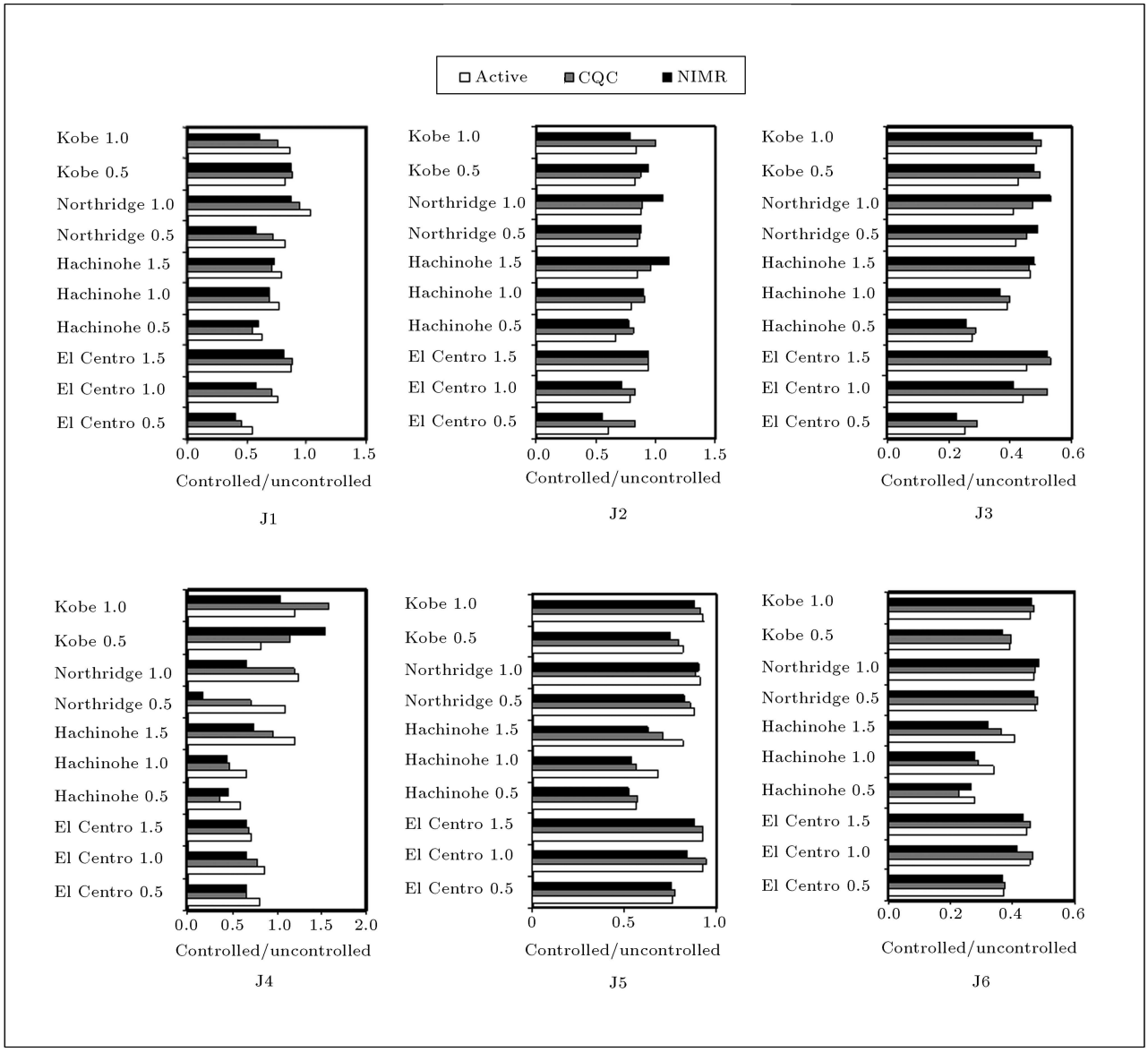

Figure 7. Comparison of performance criteria J1-J6 of NIMR to active and COC method.

and PON, but the OPC performs better than other controllers.

REFERENCES

1. Casciati, F., Magonette, G. and Marazzi, F., *Technology of Semi-Active Devices and Application in Vibration Mitigation*, John-Wiley (2006).
2. Dyke, S.J., Spencer, B.F., Jr., Sain, M.K. and Carlson, J.D. "Seismic response reduction using magnetorheological dampers", *Proc., IFAC World Congr.*, pp. 145-150 (1996c).
3. Dyke, S.J., Spencer, B.F., Jr., Sain, M.K. and Carlson, J.D. "Modeling and control of magnetorheological dampers for seismic response reduction", *Smart Mat. and Struct.*, **5**, pp. 565-575 (1996d).
4. Yoshida1, O. and Dyke, S. "Seismic control of a nonlinear benchmark building using smart dampers", *Journal of Engineering Mechanics (ASCE)*, **130**(4), pp. 386-392 (2004).
5. Bani-Hani, K.A., Mashal, A. and Sheban, M.A. "Semi-active neuro-control for base-isolation system using magnetorheological (MR) dampers", *Earthquake Engng. Struct. Dyn.*, **35**, pp. 1119-1144 (2006).
6. Jung, H.J., Lee, H.J., Yoon, W.H., Oh, J.W. and Lee, I.W. "Semiactive neurocontrol for seismic response reduction using smart damping strategy", *Journal of Computing in Civil Engineering*, **18**(3), pp. 277-280 (2004).
7. Choi, K.M., Cho, S.W., Jung, H.J. and Lee, I.W. "Semi-active fuzzy control for seismic response reduc-

tion using magnetorheological dampers", *Earthquake Engng Struct. Dyn.*, **33**, pp. 723-736 (2004).

8. Chang, C.C. and Zhou, L. "Neural network emulation of inverse dynamics for a magnetorheological damper", *Journal of Structural Engineering*, **128**(2), pp. 231-239 (2002).
9. Dyke, S.J., Yi, F. and Carlson, J.D. "Application of magnetorheological dampers to seismically excited structures", *Proc., Int. Modal Anal. Conf.*, Bethel, Conn (1999).
10. Ohtori, Y., Christenson, R.E., Spencer, B.F., Jr. and Dyke, S.J. "Benchmark control problems for seismically excited nonlinear buildings", *J. Eng. Mech.*, **130**(4), pp. 366-387 (2004).
11. Spencer, B.F., Jr., Dyke, S.J., Sain, M.K. and Carlson, J.D. "Phenomenological model of magnetorheological damper", *J. Engrg. Mech., ASCE*, **123**(3), pp. 230-238 (1997).
12. Hertz, J., Krogh, A. and Palmer, R.G., *Introduction to the Theory of Neural Computation*, Addison-Wesley Publishing Company, Boston, MA (1993).
13. *The Math Works Inc. MATLAB 7.0*, Natick, MA (2006).